

It Ain't That Bad: Understanding the Mysterious Performance Drop in OOD Generalization for Generative Transformer Models

Xingcheng Xu^{1*}, Zihao Pan^{2*}, Haipeng Zhang², Yanqing Yang^{1,3†}

Shanghai Artificial Intelligence Laboratory¹

ShanghaiTech University²

Fudan University³

xingcheng.xu18@gmail.com, {panzh,zhanghp}@shanghaitech.edu.cn, yanqingyang@fudan.edu.cn

Abstract

Generative Transformer-based models have achieved remarkable proficiency on solving diverse problems. However, their generalization ability is not fully understood and not always satisfying. Researchers take basic mathematical tasks like n -digit addition or multiplication as important perspectives for investigating their generalization behaviors. Curiously, it is observed that when training on n -digit operations (e.g., additions) in which both input operands are n -digit in length, models generalize successfully on unseen n -digit inputs (in-distribution (ID) generalization), but fail miserably and mysteriously on longer, unseen cases (out-of-distribution (OOD) generalization). Studies try to bridge this gap with workarounds such as modifying position embedding, fine-tuning, and priming with more extensive or instructive data. However, without addressing the essential mechanism, there is hardly any guarantee regarding the robustness of these solutions. We bring this unexplained performance drop into attention and ask whether it is purely from random errors. Here we turn to the mechanistic line of research which has notable successes in model interpretability. We discover that the strong ID generalization stems from structured representations, while behind the unsatisfying OOD performance, the models still exhibit clear learned algebraic structures. Specifically, these models map unseen OOD inputs to outputs with equivalence relations in the ID domain. These highlight the potential of the models to carry useful information for improved generalization.

Introduction

Transformer-based models have exhibited remarkable advancements across diverse domains, prominently in natural language processing (NLP) (Vaswani et al. 2017; Brown et al. 2020; Chowdhery et al. 2022) and fields such as computer vision (Dosovitskiy et al. 2020) and biology (Jumper et al. 2021). Among these, the extensive category of large language models, typified by instances like ChatGPT (Ouyang et al. 2022) and GPT-4 (OpenAI 2023), has demonstrated exceptional versatility, showcasing profound efficacy in tackling a myriad of tasks, ranging from natural language challenges to code translation, mathematical reasoning, and more (Bubeck et al. 2023; Trummer 2022;

Zong and Krishnamachari 2023). Although these accomplishments are undoubtedly impressive, the generalization ability of these models is not fully understood and not always satisfactory in issues such as semantic search (Asher et al. 2023), linguistic meaning capture (Bansal and Sharma 2023) and natural language understanding (Bender et al. 2021).

Given the complexity of natural language tasks and the black-box nature of these models, researchers view basic mathematical tasks such as n -digit addition or multiplication as valuable avenues for gaining insights into their generalization behaviors (Lee et al. 2023; Anil et al. 2022). Among them, many have observed an interesting yet mysterious phenomenon when training on n -digit operations (Brown et al. 2020; Anil et al. 2022; Jelassi et al. 2023). In cases where both input operands are n -digit long, the models demonstrate excellent generalization on unseen n -digit inputs. However, they unexpectedly and miserably struggle when faced with longer, unseen cases (inputs with more than n digits). For instance, when trained with operations like $349 + 705 = 1054$, the model would perform well on unseen input $350 + 705$. But when the inputs are $1349 + 2705$ which are longer in digits, the model gives a wrong answer. This creates a clear distinction between the former, known as *in-distribution (ID) generalization*, and the latter, termed *out-of-distribution (OOD) generalization*.

Seeking to bridge this generalization gap, scholars have undertaken various efforts to enhance OOD generalization. The techniques employed in this pursuit encompass a diverse spectrum, including modifying position embeddings (Jelassi et al. 2023) and attention mechanisms (Dubois et al. 2019), fine-tuning using extended data samples, prompting and Scratchpad (Anil et al. 2022), priming through selective longer-length data (Jelassi et al. 2023), and even utilizing chain-of-thought (CoT) style data (Lee et al. 2023).

In spite of these different techniques, there is still a lack of understanding regarding the underlying mechanism. The proposed solutions may therefore have questionable robustness and become vulnerable to circumstance changes (Jelassi et al. 2023). Considering the evident and notably poor OOD performance, it is natural to ask whether it stems solely from random errors or if there is anything informative learned by these models.

*These authors contributed equally.

†Corresponding author.

In this paper, we bring the mystery into attention and seek from the mechanistic perspective (Nanda and Lieberum 2022; Zhong et al. 2023) in model interpretability. This avenue of study offers a macroscopic understanding of how neural networks work and has helped identify and interpret significant phenomena such as “grokking”, also known as delayed generalization where models exhibit improved generalization long after over-fitting their training set (Liu et al. 2022).

Through training a set of lightweight generative Transformer models, including NanoGPT and MinGPT (Karpathy 2022), on n -digit addition and multiplication tasks, we have made an intriguing discovery. We find that the strong ID generalization stems from structured representations, while the models have learned a clear algebraic structure behind the unsatisfying OOD performance. Specifically, these models map unseen OOD inputs to outputs with equivalence relations in the ID domain. The representation learning process plays a crucial role in facilitating both ID and OOD generalization observed in these models. Initially, the representations are random. But as training progresses, the structure of the learned representations becomes increasingly refined, eventually allowing the models to accurately encode every input in the ID domain. Concurrently, these structured representations are continuously extended to map the unseen OOD domain. However, this extension does not occur as ideally anticipated, resulting in the poor OOD performance. Thus, the representation learning enables powerful ID generalization, but the continuous extrapolation of these representations to OOD inputs gives rise to systematic, rather than random, errors. The mechanistic insights from the discovered patterns also highlight the potential of these models to make use of the information for better generalization.

Our main contributions are as follows:

- **Showcasing the power of mechanistic empirical evaluation for LM generalization:** We train lightweight generative Transformer models (e.g. NanoGPT, MinGPT) on arithmetic tasks to directly probe ID vs OOD generalization¹, instead of resorting to workarounds. Consequently, our approach offers macroscopic insights.
- **Discovering learned structure for OOD generalization:** The discernible algebraic structure would hopefully guide robust essential solutions for strong OOD generalization.
- **Understanding the role of representations in generalization:** We show that representation learning enables strong ID performance, while unanticipated extension of representations to OOD inputs leads to systematic errors.

Related Work

Generalization of Transformer-based Models in Arithmetic

Various studies have examined the performance of Transformer-based language models in tasks involving arith-

¹Our code is available at <https://github.com/xingchengxu/ExploreGPT>

metic operations. Brown et al. (2020) investigated the ability of GPT-3 to perform basic arithmetic operations without task-specific training. Nogueira, Jiang, and Lin (2021) explored the limitations of transformers in handling simple arithmetic operations. Subsequent studies have further explored the generalization capabilities of language models in arithmetic tasks. Qian et al. (2022) discovered that language models exhibit poor OOD generalization, and traditional methods such as explicit positional markers and fine-grained computation steps do not effectively address this issue. To enhance the generalization ability of the model, certain studies have approached the issue starting from a microscopic perspective. For instance, Jelassi et al. (2023) replaced absolute position embeddings with relative position embeddings. Additionally, Dubois et al. (2019) suggested that utilizing a location-based attention mechanism proves effective in the Lookup Table task. Other research has focused on the intermediate learning process of the model. Anil et al. (2022) observed that requesting the model to generate intermediate arithmetic steps before providing the final output can improve generalization. Jelassi et al. (2023) arrived at similar conclusions by decomposing the arithmetic pipeline and improving generalization in five-digit addition tasks. In contrast, Lee et al. (2023) presented a different perspective, emphasizing the importance of high-quality, in-structive data that can quickly elicit arithmetic capabilities.

While previous studies have primarily focused on evaluating or improving the generalization capabilities of language models, our work has a different objective, we aim to uncover the underlying mechanisms that govern generalization. This explanatory goal, which seeks to understand the foundations of generalization, has not been explicitly addressed in prior research.

Mechanistic Interpretability

Neural network interpretation has seen numerous studies focusing on various types of models, including deep neural networks (DNNs) (Nam et al. 2020; Barbiero et al. 2022), convolutional neural networks (CNNs) (Yuan et al. 2019; Akhtar and Ragavendran 2020), and graph neural networks (GNNs) (Yuan et al. 2020; Xuanyuan et al. 2023). These works demonstrate diverse microscopic interpretation techniques tailored to different architectures. From a macroscopic perspective, Liu et al. (2022) tackle delayed generalization or “grokking” using addition and modular addition tasks. They provide intuitive explanations using effective theories and phase diagrams. Similarly, Zhong et al. (2023) use modular addition to mechanistically explain algorithm discovery in neural networks. Our work contributes to this growing field of mechanistic interpretability by offering a macroscopic explanation specifically for generative Transformer models.

Preliminary and Experimental Setup

Model Details

We employ the model framework of GPT, a Transformer with a decoder-only architecture comprising multiple layers

and multi-head attentions. We train several small-scale models, namely NanoGPT and MinGPT (Karpathy 2022), from random initialization using character-level tokenization and the conventional next-token prediction objective. The training is conducted on basic mathematical operations, specifically addition and multiplication of integers. Detailed hyperparameters are shown in Table 1.

Hyperparameter	Addition	Multiplication
num layer	3	6
num head	3	6
dim embd	48	192
vocab size	10	10
context window	15	19
dropout prob	0.1	0.1
optimizer	AdamW	AdamW
learning rate	0.0005	0.0005
betas	(0.9, 0.95)	(0.9, 0.95)
weight decay	0.1	0.1
grad norm clip	1.0	1.0

Table 1: Hyperparameter Information

Dataset

The dataset is structured as a concatenation of operand pairs in a natural order, with the reversed order of the operation results. This format, demonstrated to be more conducive for learning in next-token prediction models (Lee et al. 2023), offers a more approachable learning process. For instance, consider the 3-digit addition $a + b = c$, represented as “ $a_2a_1a_0 + b_2b_1b_0 = c_3c_2c_1c_0$ ” in the standard format. By reversing the output order of “ c ”, we obtain the reversed data format “ $a_2a_1a_0 + b_2b_1b_0 = c_0c_1c_2c_3$ ”. As we train addition and multiplication models as distinct entities, we omit both the operation symbols, i.e., $+$ and \times , and the equal sign, i.e., $=$, from the dataset. Subsequently, the data undergoes character-level tokenization, resulting in a vocabulary size of 10, corresponding to digits from 0 to 9. When the context window surpasses the requisite size for a 3-digit addition, we pad zeros before numbers “ a ”, “ b ”, and “ c ”. For instance, in the case of 3-digit addition with a context window of 15, the addition expression “ $349 + 705 = 1054$ ” will be encoded as “0034900705450100”.

The dataset is partitioned into three distinct subsets: the training set \mathcal{D}_1 , randomly sampled from n -digit operations; the test set \mathcal{D}_2 , also drawn from n -digit operations but intentionally devoid of any overlap with the training set (termed as the ID test set); and an additional test set \mathcal{D}_3 , sampled from m -digit operations with $m > n$, where the value at positions greater than n is non-zero (referred to as the OOD test set).

In the experiments, we set $n = 3$ and $m = 5$ for both addition and multiplication operations. Subsequently, from each of the datasets \mathcal{D}_1 , \mathcal{D}_2 , and \mathcal{D}_3 , we select 10,000 data points as the training set for addition and 50,000 for multiplication. We sample 10,000 for the ID test set and OOD test set, respectively for both operations.

ID and OOD Domains

The data space is compartmentalized into three non-overlapping regions: \mathcal{D}_1 , \mathcal{D}_2 , and \mathcal{D}_3 . The union of \mathcal{D}_1 and \mathcal{D}_2 constitutes an ID domain, whereas \mathcal{D}_3 represents an OOD domain. The models learn a function

$$f : \mathcal{D}_1 \cup \mathcal{D}_2 \cup \mathcal{D}_3 \rightarrow \mathcal{S},$$

where \mathcal{S} could be the output operation result space \mathbb{N} , the output probability space, or the learned representation space.

Since the model is exclusively trained on the \mathcal{D}_1 space, the acquired knowledge concerning \mathcal{D}_2 and \mathcal{D}_3 is an extension of \mathcal{D}_1 , albeit with an unclear underlying structure. This constitutes the core aspect we seek to understand.

Equivalence Classes

When training for addition and multiplication on n -digit operations, we have identified a discernible algebraic structure. This is encapsulated in the definition of the equivalence class $[(a, b)]_p$ for modular p , which is elucidated as follows:

$$[(a, b)]_p := \{(x, y) \in \mathbb{N}^2 \mid x \equiv a \pmod{p}, y \equiv b \pmod{p}\}.$$

The ensemble of these equivalence classes is denoted as

$$\mathbf{Z}_p^2 = \mathbf{Z}_p \times \mathbf{Z}_p = \{[(a, b)]_p \mid (a, b) \in \mathbb{N}^2\},$$

where $\mathbf{Z}_p = \mathbb{Z}/p\mathbb{Z}$ on non-negative integers.

To illustrate, when training a model on 3-digit addition, we observe that the learned operation function $f_{op} : \mathbb{N}^2 \rightarrow \mathbb{N}$ effectively translates to $f_{op}(a, b) = f_{op}([(a, b)]_{10^3})$, which will be stated in the result section.

In alternative training data scenarios, the definition of equivalence classes necessitates adaptation to accommodate specific contexts.

Results

In this section, we present the key results and findings from our experiments. These include observations on the phenomenon of generalization exhibited by the models, the learned algebraic structure, as well as the probability and representation structures in the model’s learning process.

Generalization in OOD Domain

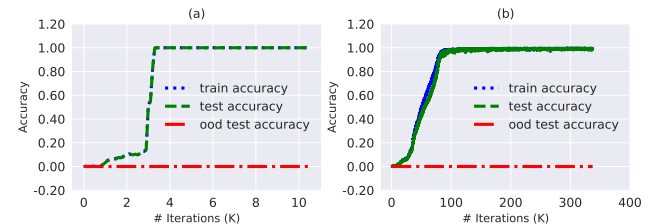


Figure 1: Training curves in addition and multiplication operations.

Figure 1 depicts the training, ID test, and OOD test accuracy for addition and multiplication operations in domains \mathcal{D}_1 , \mathcal{D}_2 , and \mathcal{D}_3 across different iterations. Panel (a) displays

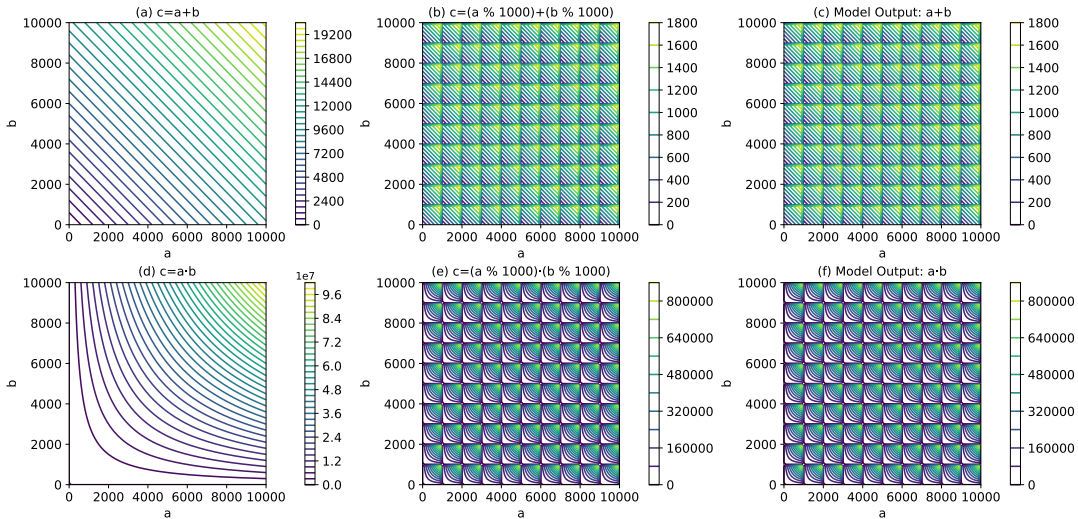


Figure 2: Contour plots for addition and multiplication operations.

the training curve for addition learned by NanoGPT, while Panel (b) showcases the curve for multiplication learned by MinGPT. The hyperparameters employed by NanoGPT and MinGPT can be found in Table 1.

By examining the figure, it becomes evident that both addition and multiplication quickly converge to a stable state, achieving (almost) 100% accuracy in training and ID testing in \mathcal{D}_1 and \mathcal{D}_2 . However, throughout the entire training process, the OOD test accuracy remains zero for both 3-digit addition and multiplication in \mathcal{D}_3 . These results align with the discoveries made by Jelassi et al. (2023) and Lee et al. (2023). When training on n -digit operations with n -digit operands, the models demonstrate excellent generalization on unseen n -digit inputs. Yet, they perform abysmally and mysteriously on longer, unseen cases, establishing a contrast between ID generalization and OOD generalization. Given the strikingly poor OOD performance, it is natural to question whether it solely stems from random errors or if there is any meaningful knowledge learned. The solution to the problem will be presented in the subsequent subsection.

Algebraic Structure

The mysterious absence of generalizability in the OOD domain prompts us to delve deeper into the results. We begin by examining some samples from domains \mathcal{D}_2 and \mathcal{D}_3 . These examples are illustrated in Table 2. When observing the 3-digit addition and multiplication cases, we notice that the trained models produce incorrect results for the 4-digit instances. Strikingly, these erroneous outputs mirror the results obtained from the 3-digit cases. It appears that the model’s outputs peculiarly “disregard” the thousands digit of the input numbers, irrespective of whether it is an addition or multiplication operation.

To systematically analyze the behavior in the OOD domain \mathcal{D}_3 , we explore the entire two-dimensional lattice of 4-digit integers, namely $\mathbb{N}^2 \cap [0, 10^4]^2$. Figure 2 presents the contour plots for the ground truth results of addition op-

Operands	Output Result	Correct Result
349 + 705	1,054	1,054
1,349 + 2,705	1,054	4,054
128 × 256	32,768	32,768
3,128 × 4,256	32,768	13,312,768

Table 2: Examples on models’ outputs for addition and multiplication.

eration $c = a + b$ (Panel (a)) and multiplication operation $c = a \cdot b$ (Panel (d)), with the number a on the horizontal axis and the number b on the vertical axis. These landscapes represent the expected learning and generalization capabilities of the models on this lattice space.

However, when we utilize our trained models to generate results based on 3-digit operations, an unmistakably distinct pattern emerges, as depicted in Panel (c) for addition and Panel (f) for multiplication. This prompts us to investigate what structure the models have learned. We discover that there is a modular relationship between the operands a and b . The learned structure can be represented as $c = (a \bmod 10^3) \circ (b \bmod 10^3)$, where \circ represents either addition $+$ or multiplication \times . The ground truth landscapes of these functions on the 4-digit integer lattice are exhibited in Panel (b) for addition and Panel (e) for multiplication. Visually, these two panels are identical to Panel (c) and Panel (f), respectively. We compare the results of the operation $(a \bmod 10^3) \circ (b \bmod 10^3)$ with the outputs produced by the model. Surprisingly, they are identical across the entire space $\mathbb{N}^2 \cap [0, 10^4]^2$.

To formalize the results, we recall the definition of equivalence classes $[(a, b)]_p$ for modular $p = 10^3$:

$$[(a, b)]_p := \{(x, y) \in \mathbb{N}^2 \mid x \equiv a \pmod{p}, y \equiv b \pmod{p}\}.$$

As $[(a, b)]_p$ is an equivalence class, we use the element in $\mathbb{N}^2 \cap [0, 10^3]^2 = \mathcal{D}_1 \cup \mathcal{D}_2$ to serve as the representative of the

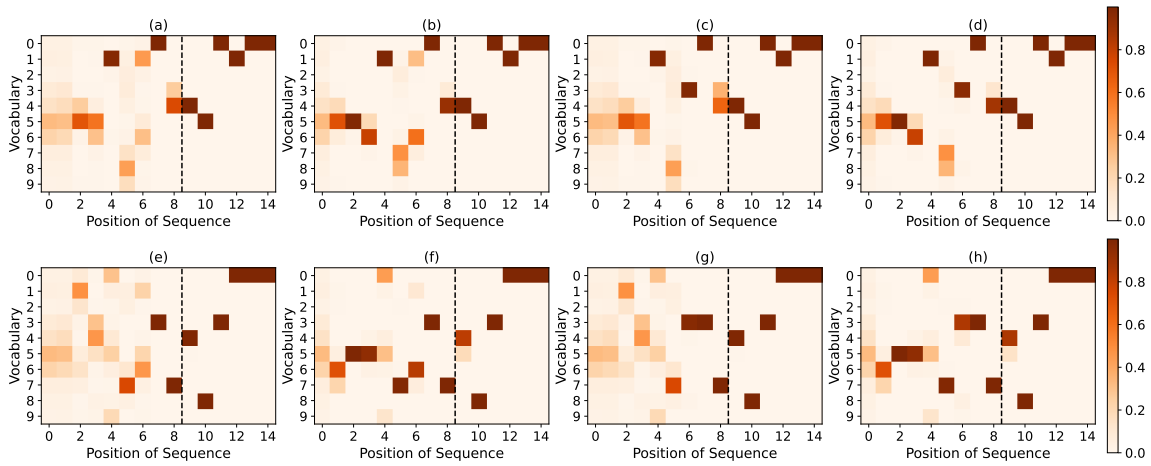


Figure 3: The probability distribution of each digit of the sequence in an addition operation $c = a + b$. The left side of the black dashed line represents the input $a + b$, while the right side is the result c . Figure 3(a) and Figure 3(e) represent the $349 + 705$ and $128 + 256$, and the outputs are 1,054 and 384 (450100 and 483000 in actual sequence output), respectively. In the second column, we perturb the thousands digit of a : Figure 3(b) represents $1,349 + 705$, and Figure 3(f) represents $3,128 + 256$. In the third column, we perturb the thousands digit of b : Figure 3(c) represents $349 + 2,705$, and Figure 3(g) represents $128 + 4,256$. In the fourth column, we simultaneously perturb the thousands digit of a and b : Figure 3(d) represents $1,349 + 2,705$, and Figure 3(h) represents $3,128 + 4,256$.

class. The ensemble of these equivalence classes then forms the space

$$\mathbf{Z}_p^2 = \mathbf{Z}_p \times \mathbf{Z}_p = \{(a, b)_p \mid (a, b) \in \mathbb{N}^2\},$$

where $\mathbf{Z}_p = \mathbb{Z}/p\mathbb{Z} = \{[0]_p, [1]_p, \dots, [p-1]_p\}$.

The models trained on 3-digit addition and multiplication actually learned the operation functions $f_{op} : \mathbf{Z}_p \times \mathbf{Z}_p \rightarrow \mathbb{N}$ for all integer pairs on $\mathbb{N} \times \mathbb{N}$ such that $f_{op}(a, b) = f_{op}([(a, b)]_p)$ with $p = 10^3$. As an example, $f_{op}(1349, 2705) = f_{op}([(349, 705)]_{10^3})$. For addition, the learned operation is $f_+(1349, 2705) = f_+([(349, 705)]_{10^3}) = 1054$, while the learned multiplication is $f_\times(1349, 2705) = f_\times([(349, 705)]_{10^3}) = 246045$.

As a summary of the results, the models learn to generalize the input in the OOD domain \mathcal{D}_3 by assimilating equivalence classes in the ID domain $\mathcal{D}_1 \cup \mathcal{D}_2$. This result shows the limitations of the models. However, this capability allows the models to extend their learned knowledge beyond the ID domain $\mathcal{D}_1 \cup \mathcal{D}_2$ shaped by the specific training data \mathcal{D}_1 . Even though the output is wrong, it is not so bad. They have still managed to acquire useful information and demonstrate some level of learning.

In order to gain a deeper understanding of the training process for Transformer models, we examine their token-level mapping using addition as an example. Consider two $(n+1)$ -digit numbers, where $a = a_n \times 10^n + \dots + a_1 \times 10 + a_0$ and $b = b_n \times 10^n + \dots + b_1 \times 10 + b_0$. When training a Transformer model using randomly sampled $(n+1)$ -digit numbers, the model learns an approximate mapping from the token-level input to the true function $c = a + b = c_{n+1} \times 10^{n+1} + \dots + c_1 \times 10 + c_0$. The learned approximation allows the model to perform classification for each digit of the resulting sum

c , as follows:

$$f_{Trans}(a_n, \dots, a_0, b_n, \dots, b_0) \approx (c_0, c_1, \dots, c_{n+1}).$$

However, if the highest digit is completely absent from the training data and is instead padded with zeros, the training only guarantees learning of low n -digit addition. In other words:

$$f_{Trans}(0, a_{n-1}, \dots, a_0, 0, b_{n-1}, \dots, b_0) \approx (c_0, c_1, \dots, c_n, 0).$$

This limitation may explain why it is challenging to generalize to higher digits when the model is trained solely on lower digits. The absence of examples with higher digits restricts the model's ability to accurately predict and generalize beyond the low-digit addition it has been trained on.

Building upon the observed algebraic structure discussed in the previous context of this subsection, we also know that when testing the Transformer models on higher digits that are non-zero, they do not significantly impact the classification of each digit of c .

As a remark, it is important to note that when dealing with alternative training data scenarios, the definition of equivalence classes may need to be adjusted accordingly. For example, if the training data consists exclusively of 1 and 3-digit operations, while OOD testing involves 2 and 4-digit numbers, or if the training data includes 3-digit numbers for operand a and 4-digit numbers for operand b , the equivalence classes would require redefining to account for these specific contexts.

Probability Structure

In the preceding subsection, we examined the structured algebraic patterns present in the output results. Considering that generative Transformer models generate outputs based

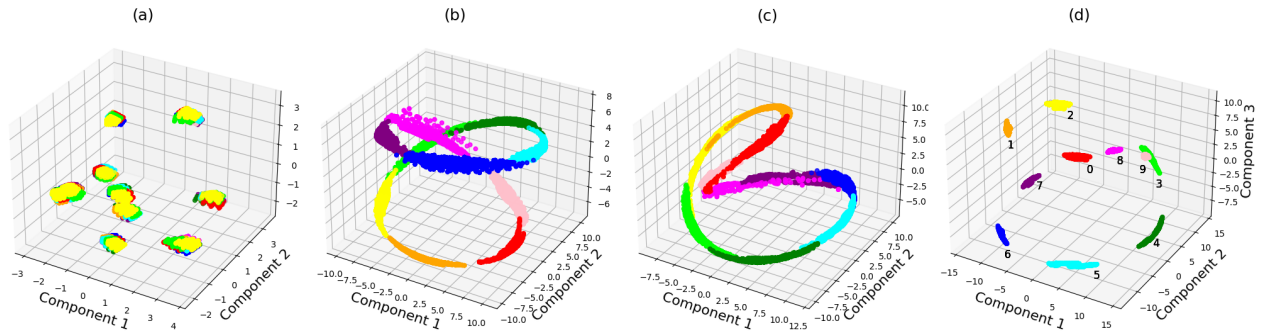


Figure 4: 3D representation structure of the first three principal components in the addition operation. Figure 4(a) to Figure 4(d) represent the initial model, model with 14%, 51%, and 100% test accuracy, respectively.

on probability distributions, our model employs a greedy approach to select the output sequence with the maximum probability. We now shift our focus from algebraic structures to the probability distribution of the output sequences. Our objective is to investigate the underlying factors that contribute to the emergence of these structured algebraic patterns.

Specifically, we take two examples of 3-digit addition, namely $a + b$. We introduce perturbations to the thousands digit of both a and b , enabling us to compare the variations in probability distributions before and after the perturbations occur. This comparative study will shed light on the mechanisms underlying the observed structured algebraic patterns.

Figure 3 displays the probability distributions of the next tokens in the vocabulary at each position within the sequence for two addition examples: $349 + 705$ and $128 + 256$. The plot showcases the probabilities before and after perturbations for each token. Remarkably, we observe that regardless of whether we perturb a and b separately or simultaneously, the probability distribution in the model’s output sequence remains largely unchanged.

Furthermore, we note that the digits with the highest probability in the output sequence remain consistent. This result implies that the algebraic structure of the model expands from $\mathbf{Z}_p \times \mathbf{Z}_p$ to $\mathbb{N} \times \mathbb{N}$. This expansion elucidates the structured patterns depicted in Figure 2. Additionally, we conducted a systematic examination of the entire integer lattice within $\mathbb{N}^2 \cap [0, 10^4]^2$. Notably, the results obtained from this comprehensive analysis exhibit robustness, further supporting our findings.

Representation Structure

Within the probability structure, we made a significant observation that the model’s output remains insensitive to perturbations in the thousands digit. This probability structure is rooted in the representation of the input sequence, which can be expressed as follows:

$$\mathbf{P} = \text{Softmax}(\mathbf{W}\mathbf{X}),$$

where $\mathbf{P} \in [0, 1]^{V \times L_{input}}$ represents the probability matrix for the next tokens at each position, $\mathbf{W} \in \mathbb{R}^{V \times d_{model}}$ signifies the learned weight matrix, and $\mathbf{X} \in \mathbb{R}^{d_{model} \times L_{input}}$ denotes the

learned representation matrix of the input. The variables V , L_{input} , and d_{model} correspond to the vocabulary size, input length, and model embedding dimension, respectively.

In this subsection, we delve deeper into the influence of these representations on the probability structure, thereby shedding light on their role in shaping the observed algebraic properties.

In order to explore the representations of $a + b$ in a systematic manner, we conducted a thorough analysis on the two-dimensional integer lattice of 4-digit numbers. Specifically, for each input sequence $a + b$, we obtained a high-dimensional embedding by considering the last column of the learned representation matrix \mathbf{X} . Subsequently, we applied principle component analysis (PCA) to project these embeddings into three or four dimensions.

Figure 4 showcases the four different phases of representation observed during the learning process of the model. The visualizations in the figure depict the representations using the first three principle components. More specifically, Figure 4(a) to 4(d) correspond to the random initial model, the model with approximately 14%, 51%, and 100% ID test accuracy, respectively. The colors in each figure correspond to the true units digit of the resulting $a + b$.

The observations made from Figure 4 demonstrate that the representations gradually transition from disorderly to structured throughout the learning process. Initially, the representations appear random with colors mixed together (Figure 4(a)). However, as the training progresses, the structure of the learned representations becomes increasingly refined (Figure 4(b) and (c)), ultimately leading to the development of a well-learned representation (Figure 4(d)) where each color is separated according to its true label.

To gain insight into the specific structures learned by the model, we focused on the final phase of representation. We selected the first four principal components of the representation using PCA, which accounted for an impressive 98.4% explained variance ratio. The contour plots of these principal components are displayed in Figure 5. Figure 5(a) to (d) showcase the first to fourth principle components of representations on the 2-dimensional integer lattice of 4-digit numbers, respectively.

Upon examining Figure 5, it becomes apparent that clear patterns emerge on each graph. Furthermore, we observe

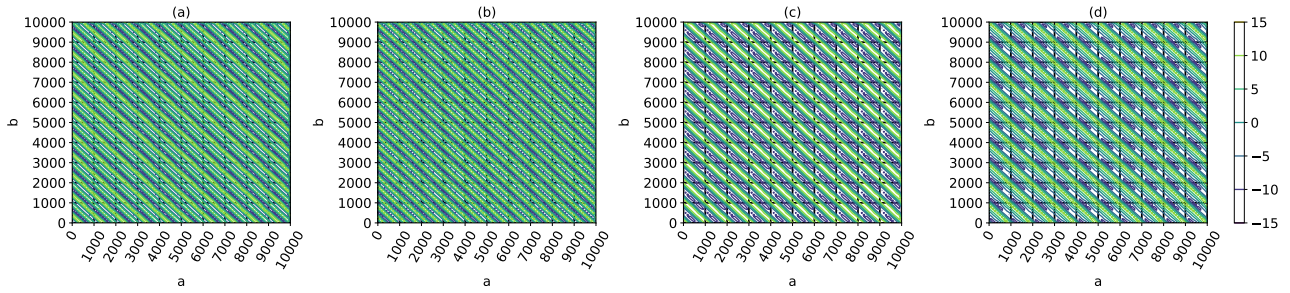


Figure 5: Representation structure of the first four principal components in the addition operation. Figure 5(a) to Figure 5(d) represent the first to the fourth principal components of model with 100% test accuracy, respectively.

that the representation structure on the entire 2-dimensional integer lattice of 4-digit numbers is similar to that observed on the lattice of 3-digit numbers. These patterns align with the algebraic structures that have been previously identified. Importantly, even when perturbing the thousands digit of the input, the representation of the input remains robust. This robustness demonstrates the model’s resilience to perturbations and reinforces the stability of the probability distribution.

From Representation to Algebraic Structure

The findings discussed above regarding algebraic structures, probability distributions, and representation structures also hold true for multiplication operations.

The systematic analysis approach outlined earlier provides a comprehensive understanding of the model’s generalization capabilities through the assimilation of equivalence classes present within the ID domain. The representation structures successfully incorporate the assimilation of these equivalence classes, thereby extending the ID structure to OOD scenarios via the probability distribution of sequences. Consequently, this assimilation becomes evident within the algebraic structures as well.

Discussion

We study the generalization behaviors of lightweight generative Transformer models, specifically in the context of arithmetic tasks. In this section, we discuss some limitations of our investigation.

Firstly, our study focused exclusively on arithmetic tasks, such as n -digit addition and multiplication problems. While arithmetic serves as a useful domain for analyzing generalization due to its structured nature, the findings may not directly translate to other types of NLP tasks or domains.

Secondly, defining ID and OOD domains for natural language is challenging. Unlike arithmetic, where the numerical values and operations define the ID domain, NLP involves a wide range of linguistic structures, vocabularies, and contextual dependencies. The boundaries between ID and OOD examples become blurred, making it difficult to precisely delineate the domains.

Moreover, determining equivalence relations in NLP tasks can be considerably more complicated. As demonstrated in

the paper, equivalence relations allow the models to map inputs based on shared characteristics or properties and thus plays a key role in the generalization behaviors observed in arithmetic. However, due to the inherent ambiguity and subjectivity of language, much more efforts may be needed to establish clear-cut equivalence relations in NLP tasks.

Conclusion

In conclusion, our study investigates the generalization behaviors of generative Transformer models trained on arithmetic tasks. Through empirical evaluation, we make several key discoveries that provide insight into their generalization abilities.

Our findings reveal that these models demonstrate strong generalization within the trained distribution, performing well on arithmetic problems within this domain. This can be attributed to the structured representations learned during training, which progressively refine to accurately encode ID inputs. However, our investigation also uncovers an underlying algebraic structure that contributes to the models’ unsatisfactory performance on OOD inputs. The models attempt to map OOD inputs using equivalence relations within the ID domain, leading to errors and a lack of robustness in OOD scenarios. The representation learning process plays a crucial role in enabling both ID and OOD generalization. While representations become refined for ID inputs, extending them to OOD inputs does not occur optimally, resulting in suboptimal performance.

Despite challenges in OOD generalization, our findings suggest that these models hold valuable information for improved generalization. The structured representations offer crucial insights that, if utilized effectively, could enhance the models’ capabilities and improve OOD performance. To advance generalization capabilities further, novel strategies could be explored to address the issues raised in this study, including optimizing representation extension, reducing systematic errors, and promoting robust performance.

References

Akhtar, N.; and Ragavendran, U. 2020. Interpretation of intelligence in CNN-pooling processes: a methodological survey. *Neural computing and applications*, 32(3): 879–898.

Anil, C.; Wu, Y.; Andreassen, A.; Lewkowycz, A.; Misra, V.; Ramasesh, V.; Slone, A.; Gur-Ari, G.; Dyer, E.; and

- Neyshabur, B. 2022. Exploring length generalization in large language models. *Advances in Neural Information Processing Systems*, 35: 38546–38556.
- Asher, N.; Bhar, S.; Chaturvedi, A.; Hunter, J.; and Paul, S. 2023. Limits for Learning with Language Models. *arXiv preprint arXiv:2306.12213*.
- Bansal, P.; and Sharma, A. 2023. Large Language Models as Annotators: Enhancing Generalization of NLP Models at Minimal Cost. *arXiv preprint arXiv:2306.15766*.
- Barbiero, P.; Ciravegna, G.; Giannini, F.; Lió, P.; Gori, M.; and Melacci, S. 2022. Entropy-based logic explanations of neural networks. In *Proceedings of the AAAI Conference on Artificial Intelligence*, volume 36, 6046–6054.
- Bender, E. M.; Gebru, T.; McMillan-Major, A.; and Shmitchell, S. 2021. On the dangers of stochastic parrots: Can language models be too big? In *Proceedings of the 2021 ACM conference on fairness, accountability, and transparency*, 610–623.
- Brown, T.; Mann, B.; Ryder, N.; Subbiah, M.; Kaplan, J. D.; Dhariwal, P.; Neelakantan, A.; Shyam, P.; Sastry, G.; Askell, A.; et al. 2020. Language models are few-shot learners. *Advances in neural information processing systems*, 33: 1877–1901.
- Bubeck, S.; Chandrasekaran, V.; Eldan, R.; Gehrke, J.; Horvitz, E.; Kamar, E.; Lee, P.; Lee, Y. T.; Li, Y.; Lundberg, S.; et al. 2023. Sparks of artificial general intelligence: Early experiments with GPT-4. *arXiv preprint arXiv:2303.12712*.
- Chowdhery, A.; Narang, S.; Devlin, J.; Bosma, M.; Mishra, G.; Roberts, A.; Barham, P.; Chung, H. W.; Sutton, C.; Gehrmann, S.; et al. 2022. PALM: Scaling language modeling with pathways. *arXiv preprint arXiv:2204.02311*.
- Dosovitskiy, A.; Beyer, L.; Kolesnikov, A.; Weissenborn, D.; Zhai, X.; Unterthiner, T.; Dehghani, M.; Minderer, M.; Heigold, G.; Gelly, S.; et al. 2020. An image is worth 16x16 words: Transformers for image recognition at scale. *arXiv preprint arXiv:2010.11929*.
- Dubois, Y.; Dagan, G.; Hupkes, D.; and Bruni, E. 2019. Location attention for extrapolation to longer sequences. *arXiv preprint arXiv:1911.03872*.
- Jelassi, S.; d’Ascoli, S.; Domingo-Enrich, C.; Wu, Y.; Li, Y.; and Charton, F. 2023. Length Generalization in Arithmetic Transformers. *arXiv preprint arXiv:2306.15400*.
- Jumper, J.; Evans, R.; Pritzel, A.; Green, T.; Figurnov, M.; Ronneberger, O.; Tunyasuvunakool, K.; Bates, R.; Židek, A.; Potapenko, A.; et al. 2021. Highly accurate protein structure prediction with AlphaFold. *Nature*, 596(7873): 583–589.
- Karpathy, A. 2022. A minimal PyTorch re-implementation of the OpenAI GPT (Generative Pretrained Transformer) training. *GitHub* <https://github.com/karpathy/minGPT>.
- Lee, N.; Sreenivasan, K.; Lee, J. D.; Lee, K.; and Papailiopoulos, D. 2023. Teaching Arithmetic to Small Transformers. *arXiv preprint arXiv:2307.03381*.
- Liu, Z.; Kitouni, O.; Nolte, N. S.; Michaud, E.; Tegmark, M.; and Williams, M. 2022. Towards understanding grokking: An effective theory of representation learning. *Advances in Neural Information Processing Systems*, 35: 34651–34663.
- Nam, W.-J.; Gur, S.; Choi, J.; Wolf, L.; and Lee, S.-W. 2020. Relative attributing propagation: Interpreting the comparative contributions of individual units in deep neural networks. In *Proceedings of the AAAI conference on artificial intelligence*, volume 34, 2501–2508.
- Nanda, N.; and Lieberum, T. 2022. A mechanistic interpretability analysis of grokking. In *Alignment Forum*.
- Nogueira, R.; Jiang, Z.; and Lin, J. 2021. Investigating the limitations of transformers with simple arithmetic tasks. *arXiv preprint arXiv:2102.13019*.
- OpenAI. 2023. GPT-4 Technical Report. *ArXiv*, abs/2303.08774.
- Ouyang, L.; Wu, J.; Jiang, X.; Almeida, D.; Wainwright, C.; Mishkin, P.; Zhang, C.; Agarwal, S.; Slama, K.; Ray, A.; et al. 2022. Training language models to follow instructions with human feedback. *Advances in Neural Information Processing Systems*, 35: 27730–27744.
- Qian, J.; Wang, H.; Li, Z.; Li, S.; and Yan, X. 2022. Limitations of language models in arithmetic and symbolic induction. *arXiv preprint arXiv:2208.05051*.
- Trummer, I. 2022. CodexDB: Synthesizing code for query processing from natural language instructions using GPT-3 Codex. *Proceedings of the VLDB Endowment*, 15(11): 2921–2928.
- Vaswani, A.; Shazeer, N.; Parmar, N.; Uszkoreit, J.; Jones, L.; Gomez, A. N.; Kaiser, Ł.; and Polosukhin, I. 2017. Attention is all you need. *Advances in neural information processing systems*, 30.
- Xuanyuan, H.; Barbiero, P.; Georgiev, D.; Magister, L. C.; and Lió, P. 2023. Global concept-based interpretability for graph neural networks via neuron analysis. In *Proceedings of the AAAI Conference on Artificial Intelligence*, volume 37, 10675–10683.
- Yuan, H.; Chen, Y.; Hu, X.; and Ji, S. 2019. Interpreting deep models for text analysis via optimization and regularization methods. In *Proceedings of the AAAI Conference on Artificial Intelligence*, volume 33, 5717–5724.
- Yuan, H.; Tang, J.; Hu, X.; and Ji, S. 2020. Xggn: Towards model-level explanations of graph neural networks. In *Proceedings of the 26th ACM SIGKDD International Conference on Knowledge Discovery & Data Mining*, 430–438.
- Zhong, Z.; Liu, Z.; Tegmark, M.; and Andreas, J. 2023. The Clock and the Pizza: Two Stories in Mechanistic Explanation of Neural Networks. *arXiv preprint arXiv:2306.17844*.
- Zong, M.; and Krishnamachari, B. 2023. Solving math word problems concerning systems of equations with GPT-3. In *Proceedings of the AAAI Conference on Artificial Intelligence*, volume 37, 15972–15979.